Analytical Methods

PAPER

View Article Online
View Journal

Cite this: DOI: 10.1039/c5ay00776c

Fragmentation patterns of five types of phospholipids by ultra-high-performance liquid chromatography electrospray ionization quadrupole time-of-flight tandem mass spectrometry

Juanjuan Pi, Xia Wu and Yifan Feng*

Fragmentation patterns of phospholipids have been thoroughly investigated in previous studies. However, most studies only concentrate on these patterns for several phospholipids in single ion mode (positive or negative ion mode); this has not provided a systematic summarization for more phospholipids. Because phospholipidomics studies require high throughput screening of the target phospholipids, the necessity for rapid identification schemes for these compounds becomes obvious. Fragmentation patterns of five major types of phospholipids, including phosphatidylcholine (PC), phosphatidylethanolamine (PE), phosphatidylserine (PS), phosphatidylinositol (PI) and sphingomyelins (SM), in different ion modes at several elevated collision energies (10–50 eV) have been studied by ultra-high-performance liquid chromatography electrospray ionization quadrupole time-of-flight tandem mass spectrometry (UHPLC/ESI-Q-TOFMS). The different characteristic ions of phospholipids in ESI (±) modes, three possible patterns ($[RC{=}O]^+$, $[RCOO^-]^-$, and neutral ion R′CH=CO) of fatty acyl chains in ESI (±) modes, and changes in the abundance ratios of the *sn*-1/*sn*-2 carboxylate anions of phospholipids at different collision energies, which can be used to quickly identify the positions of fatty acyl chains of phospholipids, were revealed. Fragmentation patterns of five major types of phospholipids were systematically summarized. This summary provides reference tools for the rapid identification of phospholipids and the opportunity to obtain complementary and more comprehensive results in future phospholipidomics studies.

Received 24th March 2015
Accepted 23rd December 2015

DOI: 10.1039/c5ay00776c

www.rsc.org/methods

1 Introduction

Phospholipids are often classified in two categories: glycerophospholipids, which exist widely in living beings, and sphingomyelins (SM). Glycerophospholipids, whose nomenclature involves stereospecific numbering (*sn*), consist of a glycerol backbone with alkylation or acylation at the *sn*-1 and/or *sn*-2 positions and a phosphate ester at the *sn*-3 position.[1] The various fatty acyl substituents linked at the *sn*-1 and/or *sn*-2 carbons enrich the molecular diversity of each kind of glycerophospholipid. The *sn*-3 carbon participates in phosphodiester linkages to different polar head groups, which enables the tentative classification of glycerophospholipids into five major types: phosphatidylcholine (PC), phosphatidylethanolamine (PE), phosphatidylserine (PS), phosphatidylinositol (PI) and phosphatidylglycerol (PG). Phospholipids play important roles in components of cell membranes, membrane fusion, signal transduction and receptor ligands.[2–7] Furthermore, an increasing number of recent studies have indicated that the pathogenesis of numerous human chronic diseases, such as diabetes and obesity, may be caused by metabolism disorders involving phospholipids.[8–11] Thus, research into phospholipids, such as phospholipidomics, is attracting increasing interest.[12–14] It could be a challenging task to analyze phospholipids, since they exist largely in cells or living beings as a mixture of molecules with similar structures, wide concentration ranges and different polarities. Before the popular use of mass spectrometry (MS), thin layer chromatography and gas chromatography were the main analytical methods; these could only be used to detect a molecule of a specific class or with a specific fatty acyl chain, and could not be applied to identify all molecules in a phospholipid mixture.[15–18] New possibilities in the research of phospholipids have been opened up by the development of high resolution mass spectrometry (such as Q-TOFMS), especially fragmentation patterns, which can be used to identify the molecular structures of phospholipids.[19] Erlend Hvattum *et al.* have discussed the fragmentation pathway of phosphatidylserine in negative ESI mode, and Yan

Central Laboratory, Guangdong Pharmaceutical University, No. 280, East Rd of Outer Ring in College Station, Panyu District, Guangzhou City, Guangdong Province, China. E-mail: tfengyf@163.com

Xiaojun *et al.* have roughly summarized the characteristic daughter ions of glycerophospholipids in negative ESI mode.[20,21] However, these studies of fragmentation patterns concentrated on several kinds of phospholipids or a single ion mode (positive or negative ion mode) only;[20,21] the common patterns of most phospholipids in all ion modes were not summarized systematically, which is necessary for the rapid identification of target phospholipids in high throughput screening, especially for phospholipidomics studies.

Herein, UHPLC/ESI-Q-TOFMS was utilized to analyze mixed standards of five phospholipid compositions. The fragmentation patterns of five major types of phospholipids (PE, PI, PC, PS and SM) were studied systematically in different ion modes at several elevated collision energies (10 to 50 eV). Combined with our previous research,[22,23] all the fragmentation patterns were summarized, including different characteristic ions of phospholipids in different ion modes, three patterns ($[RC{=}O]^+$, $[RCOO^-]^-$ and R′CH=CO) of common fatty acyl chain ions of glycerophospholipids in different ion modes, and the variation trend of the ratios of *sn*-1/*sn*-2 carboxylate ions in ESI (−) mode at different collision energies (10 to 50 eV), which could be used to rapidly identify possible phospholipids according to their MS and MS/MS information.

2 Experimental

2.1 Chemicals and reagents

Acetonitrile, methanol and isopropanol of HPLC grade were obtained from Merck (Germany), acetic acid (HPLC-grade) from Aladdin Technologies, and leucine-enkephalin was obtained from Sigma-Aldrich (USA). Chloroform, hydrochloric acid and ammonium acetate (analytical reagent) were

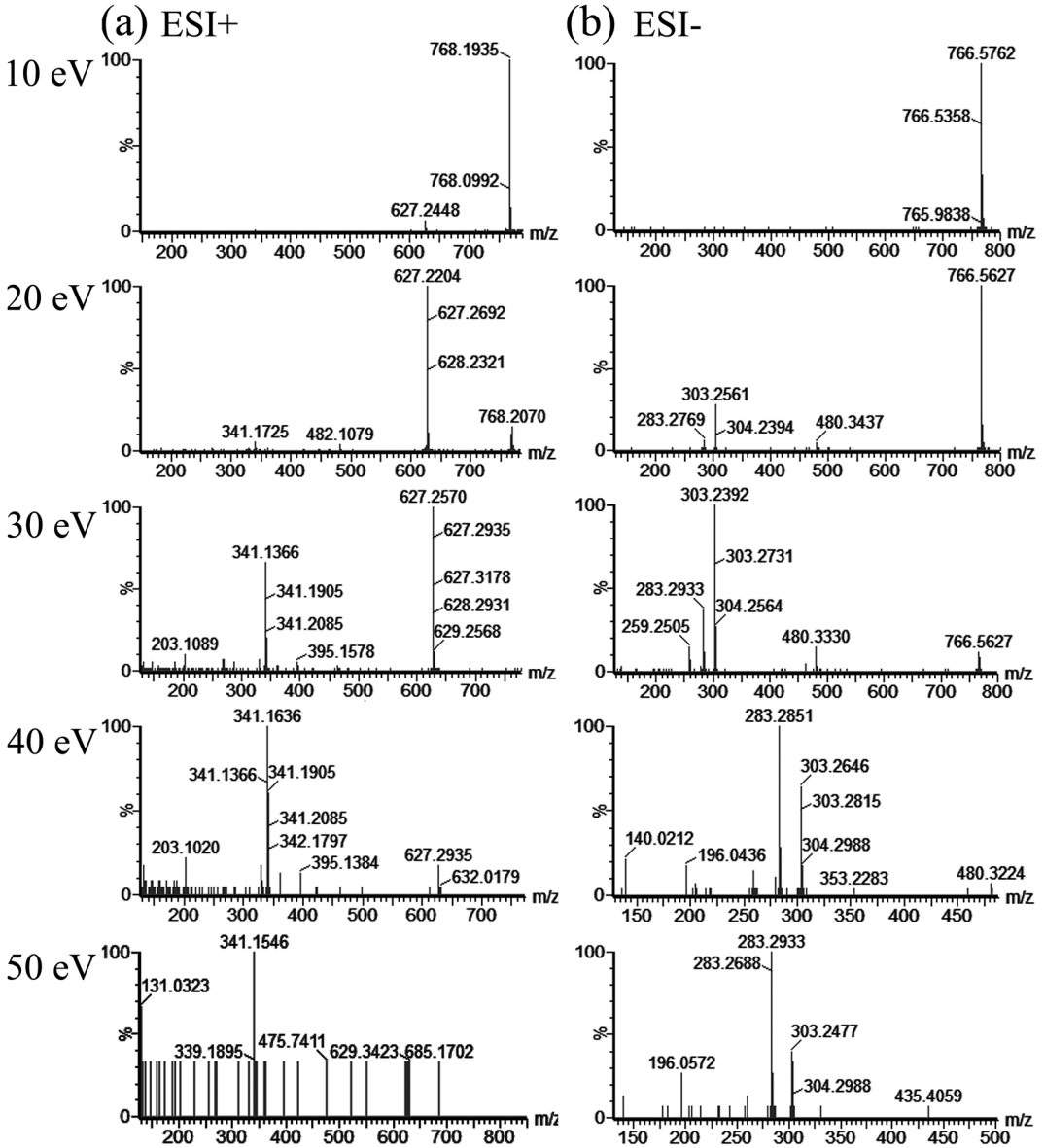

Fig. 1 MS/MS spectra of PE (18 : 0/20 : 4) in ESI (+) (a) and ESI (−) (b) modes at different collision energies (10 eV, 20 eV, 30 eV, 40 eV, and 50 eV).

purchased from Fuyu Specialty Chemical Co. Ltd (China). Doubly distilled water provided by Watson's Food & Beverage (China) was used as the solvent throughout the experiments. PE (18 : 0/20 : 4,5*Z*,8*Z*,11*Z*,14*Z*), PI (18 : 0/20 : 4,5*Z*,8*Z*,11*Z*,14*Z*), PS (16 : 0/18 : 1,9*Z*), PC (18 : 0/18 : 2,6*Z*,9*Z*) and SM (d18 : 1/18 : 0) standards were purchased from Avanti Polar Lipids Inc (USA).

2.2 Preparation of the standards

Each standard was prepared as a 5 mg mL^{-1} mother liquor with chloroform. 10 μL mother liquors were drawn and mixed in a 5 mL volumetric flask, and the mixture was constant-volume processed with methanol.

2.3 UHPLC conditions

An ACQUITY UHPLC/Q-TOFMS system (Waters, USA) equipped with a binary pump, vacuum degasser and autosampler was controlled with MassLynx™ (V4.1) software. Separation was performed at 50 °C on an ACQUITY UHPLC BEH C18 column (2.1 mm × 50 mm, 1.7 μm; Waters). The mobile phases consisted of water containing 10 mM ammonium acetate and 0.1% acetic acid (A), and 50% acetonitrile–isopropanol (v/v) containing 10 mM ammonium acetate and 0.1% acetic acid (B) with a flow rate of 0.3 mL min^{-1}. A gradient elution program was set as follows: 60% to 81.4% B at 0 to 4 min, 81.4% to 90% B at 4–20 min.[22]

2.4 MS conditions

The ACQUITY UHPLC/Q-TOFMS system was equipped with an ESI ion source operating in positive ion mode (ESI+) and negative ion mode (ESI−). The spectra were acquired in the range of *m*/*z* 420 to 950 for full scan time MS analysis and *m*/*z* 80 to 800 for MS/MS analysis. High-purity nitrogen (N_2) was used as the desolvation gas at a flow rate of 500 L h^{-1}, and ultrahigh-purity helium (He) was used as the collision gas. The flow rate of the cone gas (N_2) was 50 L h^{-1}. The desolvation and source

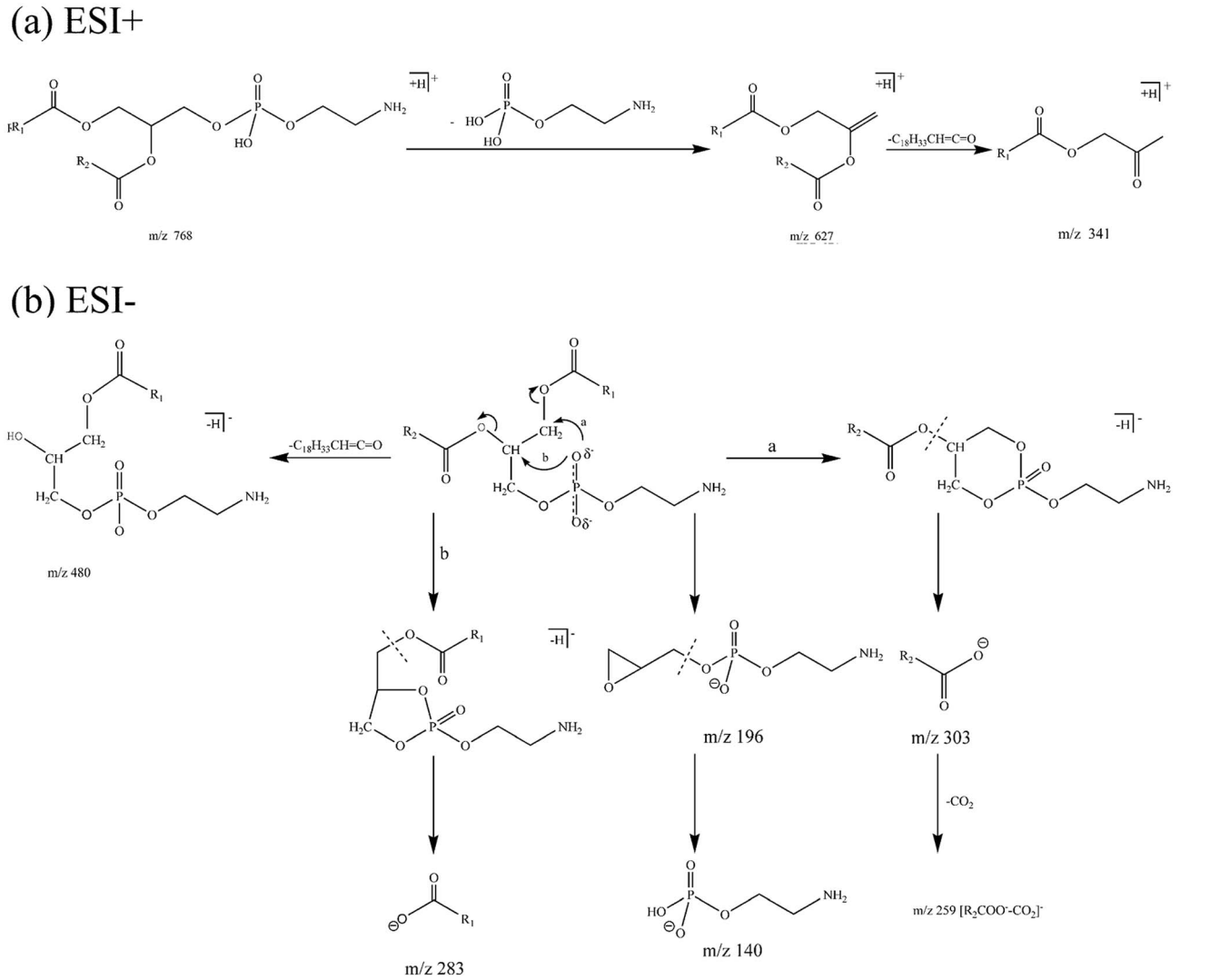

Fig. 2 The fragmentation pathways of PE (18 : 0/20 : 4) in ESI (+) (a) and ESI (−) (b) modes.

temperatures were 350 °C and 120 °C, respectively. The cone voltage was 3000 V, the capillary voltage was 2300 V for ESI (±) and the sample cone voltage was 30 V. The MS/MS analysis was performed using variable collision energies (10, 20, 30, 40 and 50 eV). To ensure accuracy during the MS analysis, the acquired data was corrected *via* an external reference (Lock-Spray™) consisting of leucine-enkephalin with $[M + H]^+ = 556.2771$ in ESI (+) and $[M - H]^- = 554.2615$ in ESI (−). All data collected in ESI (+) and ESI (−) modes were acquired using the MassLynx™ (V4.1) software system.

3 Results and discussion

3.1 The fragmentation regularities of PE and PI

The fragmentation patterns of standard PE (18 : 0/20 : 4) and PI (18 : 0/20 : 4) at different MS^2 collision energies (10–50 eV) were investigated in ESI (+) mode, as shown in Fig. 1a and 2a. At the collision energies of 10 and 20 eV, PE (18 : 0/20 : 4) predominantly formed ions at *m*/*z* 768 $[M + H]^+$ and further lost its polar head group to produce ions at *m*/*z* 627 $[M + H - 141]^+$. The ion $[M + H - 141]^+$ was considered as the characteristic ion of PE in ESI (+) mode.[24] The ions at *m*/*z* 341 $[M + H - 141 - C_{18}H_{33}CHCO]^+$ arose from the precursor ions at *m*/*z* 627 by the loss of a neutral ion ($C_{18}H_{33}CHCO$) when the collision energies exceeded 30 eV. Synchronously, minor intensity ions at *m*/*z* 482 $[M + H - C_{18}H_{33}CHCO]^+$ were detected. In the fragmentation of standard PI (18 : 0/20 : 4), molecular ions at *m*/*z* 887 $[M + H]^+$ were formed. The molecular ions then produced ions at *m*/*z* 627 $[M + H - H_2PO_4\text{-}CH(CH(OH))_5]^+$ after losing their phosphate head groups, and further formed daughter ions at *m*/*z* 341 $[627 - C_{18}H_{33}CHCO]^+$

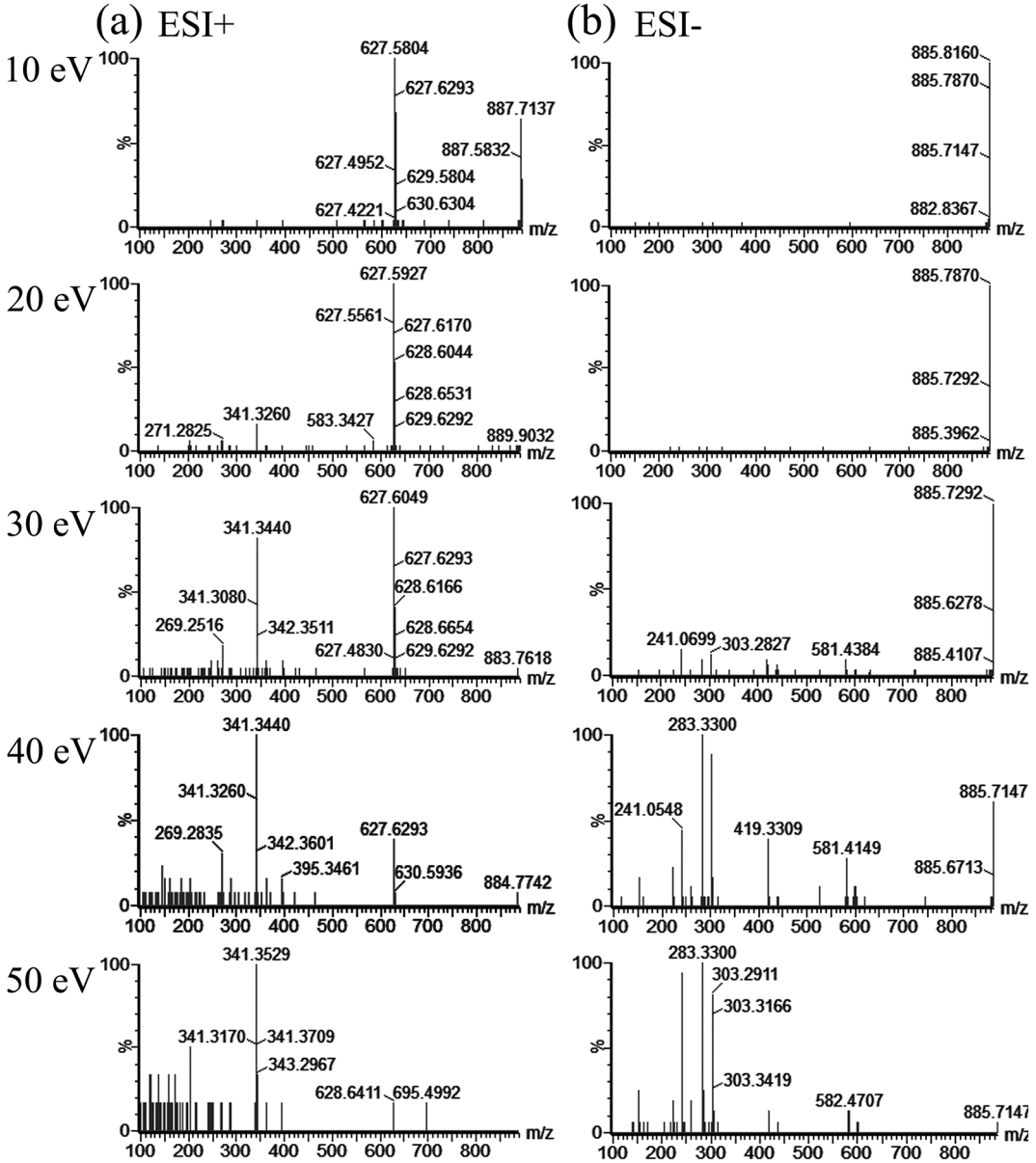

Fig. 3 MS/MS spectra of PI (18 : 0/20 : 4) in ESI (+) (a) and ESI (−) (b) modes at different collision energies (10 eV, 20 eV, 30 eV, 40 eV, and 50 eV).

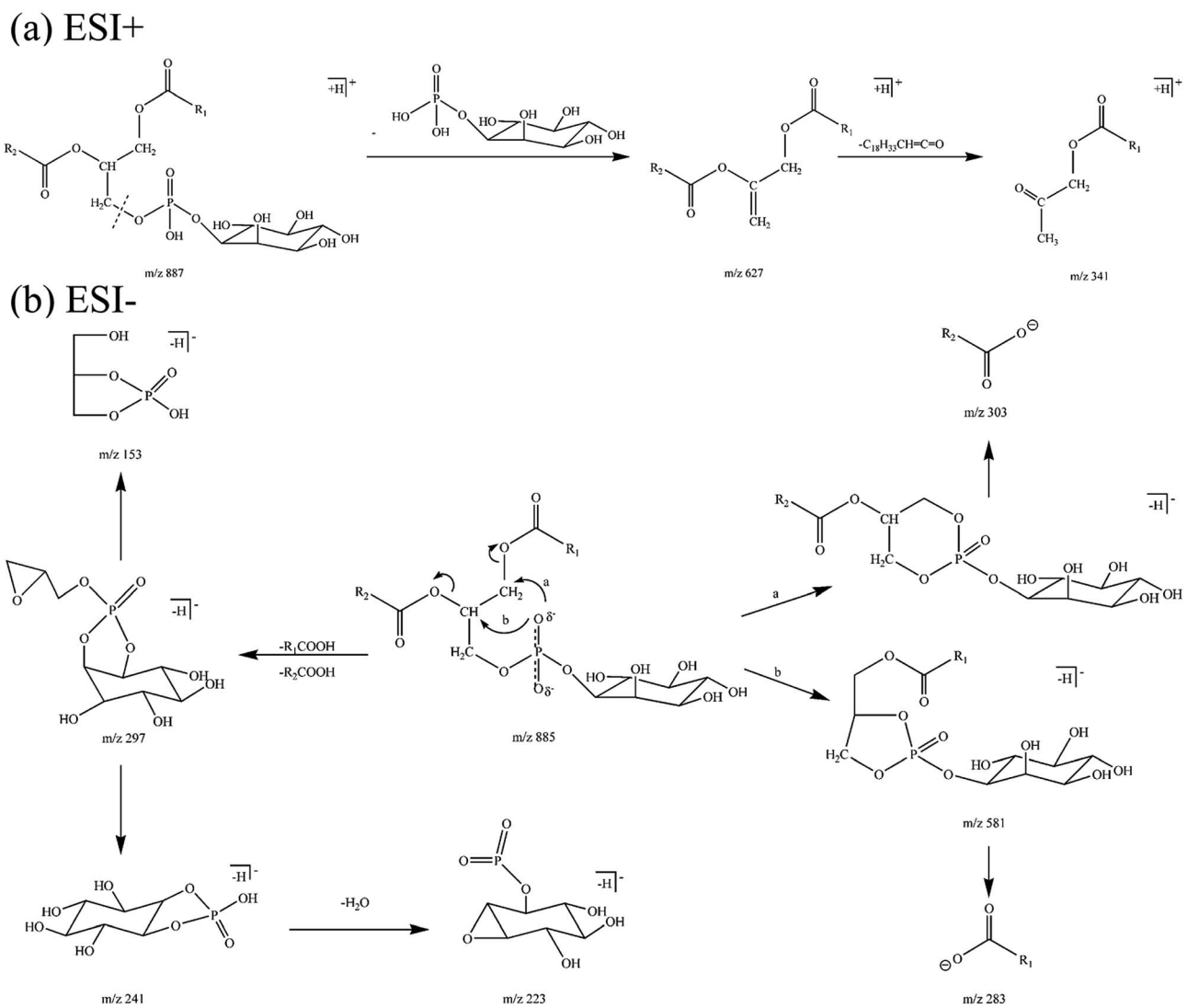

Fig. 4 The fragmentation pathways of PI (18 : 0/20 : 4) in ESI (+) (a) and ESI (−) (b) modes.

following the cleavage of the *sn*-2 ester bond. The fragmentation pathways of PE and PI under ESI (+) are shown in Fig. 3a and 4a.

In ESI (−) mode, daughter ions at *m*/*z* 303 $[R_2COO^-]^-$, 259 $[R_2COO^- - CO_2]^-$, 283 $[R_1COO^-]^-$, 480 $[M - H - C_{18}H_{33}CHC{=}O]^-$, and characteristic ions at *m*/*z* 140 $[C_2H_7O_4NP]^-$ and *m*/*z* 196 $[C_5H_{11}O_5NP]^-$ were formed, in addition to the molecular ions at *m*/*z* 766 $[M - H]^-$ of PE (18 : 0/20 : 4).[21] In the fragmentation of PI (18 : 0/20 : 4), the molecular ions at *m*/*z* 885 $[M - H]^-$ produced daughter ions at *m*/*z* 581 $[M - H - R_2COOH]^-$, *m*/*z* 303 $[R_2COO^-]^-$, *m*/*z* 283 $[R_1COO^-]^-$ and *m*/*z* 241 $[C_6H_{10}O_8P]^-$ by the cleavages of ester bonds and the polar head group. Then the daughter ions produced ions at *m*/*z* 419 $[581 - C_6H_{10}O_5]^-$, *m*/*z* 223 $[241 - H_2O]^-$, *m*/*z* 297 $[C_9H_{14}O_9P]^-$ and *m*/*z* 153 $[C_3H_6O_5P]^-$ after further fragmentation. Among these, the ion at *m*/*z* 241 $[C_6H_{10}O_8P]^-$ is the characteristic ion of PI, which could be used to distinguish PI in biological samples or pharmaceutical products, and the ion at *m*/*z* 153 $[C_3H_6O_5P]^-$ is the characteristic ion of all the glycerophospholipids. Their fragmentation pathways are shown in Fig. 3b and 4b. Interestingly, as shown in Fig. 1b and 2b, the *sn*-1/*sn*-2 carboxylate anions of PE (18 : 0/20 : 4) and PI (18 : 0/20 : 4) at different collision energies had similar abundance ratios.[25,26] The $[R_2COO^-]^-$ signal was higher than that of $[R_1COO^-]^-$ (*sn*-1/*sn*-2 < 1) of PE (18 : 0/20 : 4) and PI (18 : 0/20 : 4) at collision energies of 20 to 30 eV, and lower than that of $[R_1COO^-]^-$ (*sn*-1/*sn*-2 > 1) at collision energies of 40 to 50 eV. Structurally, PE (18 : 0/20 : 4) and PI (18 : 0/20 : 4) have different polar head groups and the same hydrophobic fatty acyl chain. Thus, it was considered that the different structure of the polar head groups of PE (18 : 0/20 : 4) and PI (18 : 0/20 : 4) contributed equally to the ratio of the *sn*-1/*sn*-2 carboxylate anions. The fragmentation of two acyl chains of glycerophospholipids leading to the formation of the *sn*-1 and *sn*-2 carboxylate anions was possibly due to an attack of the anionic site of the phosphate group from path a or b, involving a six- or five-membered ring transition state

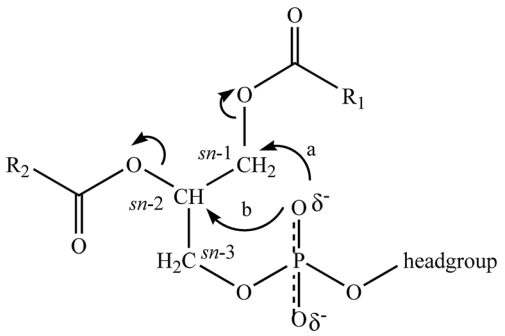

Fig. 5 Mechanism leading to the formation of *sn*-1 and *sn*-2 carboxylate ions from glyceryl phospholipids in ESI (−) mass spectrometry (adapted from study by Vernooij[25]).

(see Fig. 5), respectively.[27] Apparently, the abundance ratios of the carboxylate anions of PE (18 : 0/20 : 4) and PI (18 : 0/20 : 4) depend mainly upon the stability of the cyclic phosphate ester and the steric hindrance of the head group structure.[27] The attack of the phosphate anion at C-1 of the glycerol backbone is unfavourable if there is steric hindrance from the phospholipid head group at low collision energies (20 to 30 eV).[28] PE forms intramolecular hydrogen bonds between its primary amine and carbonyl groups, while PI has an inositol group, restricting the attack from path a at low collision energies.[20,25,29] When the collision energy increases, the six-membered ring transition state preferentially forms. The above findings indicate that the anionic sites of the phosphate groups of PE (18 : 0/20 : 4) and PI (18 : 0/20 : 4) tend to form five-membered rings (which produces the *sn*-2 carboxylate anions at *m*/*z* 303 $[R_2COO^-]^-$) at low collision energies (20 to 30 eV), and six-membered rings at high collision energies (40 to 50 eV) (which produces the *sn*-1 carboxylate anions at *m*/*z* 283 $[R_1COO^-]^-$). Therefore, the characteristic ions of PE and PI could be used for qualitative identification, and the abundance ratios of the *sn*-1/*sn*-2 carboxylate anions at different collision energies could be used to identify the positions of the two fatty acyl chains (see Table 1).

Table 1 Characteristic ions and neutral loss of different phospholipids in different ESI modes

	ESI (+)		ESI (−)		
Type	Fragment structure	*m*/*z*	Fragment structure	*m*/*z*	*sn*-1/*sn*-2, (collision energy, eV)
All glycerophospholipids			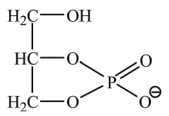	153	
PE	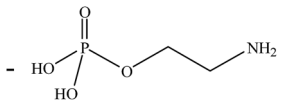	$[M + H - 141]^+$	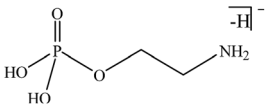	140	<1, (20–30 eV) >1, (40–50 eV)
			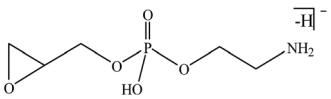	196	
PI			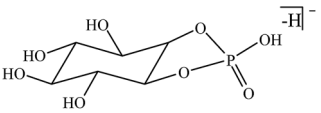	241	<1, (20–30 eV) >1, (40–50 eV)
PC	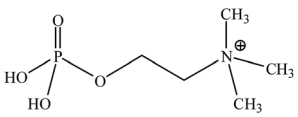	184	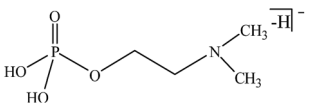	168	<1, (20–50 eV)
PS	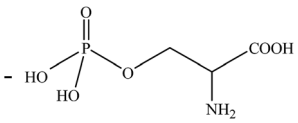	$[M + H - 185]^+$	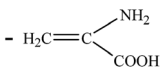	$[M - H - 87]^-$	>1, (20–50 eV)
SM	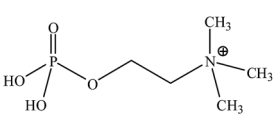	184	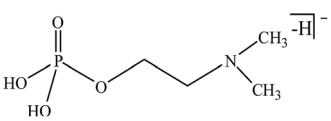	168	

3.2 The fragmentation regularities of PC and PS

PC, known as lecithin, readily forms molecular ions $[M + H]^+$ and adduct molecular ions $[M + Na]^+$ if the mobile phase contains alkali metals (Na^+, *etc.*) in ESI (+) mode.[30] In ESI (+) mode, standard PC (18 : 0/18 : 2) formed the ions at *m/z* 786 $[M + H]^+$ and characteristic ions at *m/z* 184 $[C_5H_{15}O_4NP]^+$.[31,32] When the collision energies were set at 30, 40 and 50 eV, daughter ions at *m/z* 603 $[M - HPO_4CH_2CH_2N(CH_3)_3]^+$, *m/z* 524 $[M + H - C_{16}H_{29}CH{=}C{=}O]^+$, *m/z* 506 $[524 - H_2O]^+$, *m/z* 502 $[M + H - C_{16}H_{33}CH{=}C{=}O - H_2O]^+$ and *m/z* 341 $[M - HPO_4\text{-}CH_2CH_2N(CH_3)_3 - C_{16}H_{29}CHC{=}O]^+$ were detected (see Fig. 6a and 7a). In the fragmentation of standard PS (16 : 0/18 : 1), the characteristic daughter ions at *m/z* 577 $[M + H - 185]^+$ derived from the molecular ion at *m/z* 762 $[M + H]^+$ by losing the phosphate head group.[21] Simultaneously, the other daughter ions at *m/z* 239 $[C_{15}H_{29}C{=}O]^+$, *m/z* 265 $[C_{17}H_{33}C{=}O]^+$, *m/z* 313 $[M + H - C_{16}H_{32}CH{=}C{=}O]^+$ and *m/z* 339 $[M + H - C_{14}H_{28}CHC{=}O]^+$ were detected (see Fig. 8a and 9a).

In ESI (−) mode, the characteristic ions at *m/z* 168 $[C_4H_{11}O_4NP]^-$ and *m/z* 673 $[M - H - 87]^-$ of PC (18 : 0/18 : 2) and PS (16 : 0/18 : 1) were found, respectively, in addition to their other daughter ions (see Fig. 7b and 9b).[21,33,34] In contrast with PE and PI, the abundance ratios of the *sn*-1/*sn*-2 carboxylate anions of PC and PS did not change; the ratio of the *sn*-1/*sn*-2 carboxylate anions of PC was less than 1 at collision energies of 20 to 50 eV (see Fig. 6b), while the ratio of PS was greater than 1 at collision energies of 20 to 50 eV (see Fig. 8b). As shown in Fig. 5, PC preferentially formed a five-membered ring and produced a higher intensity of ions at *m/z* 279 $[R_2COO^-]^-$; it is believed that steric hindrance of the

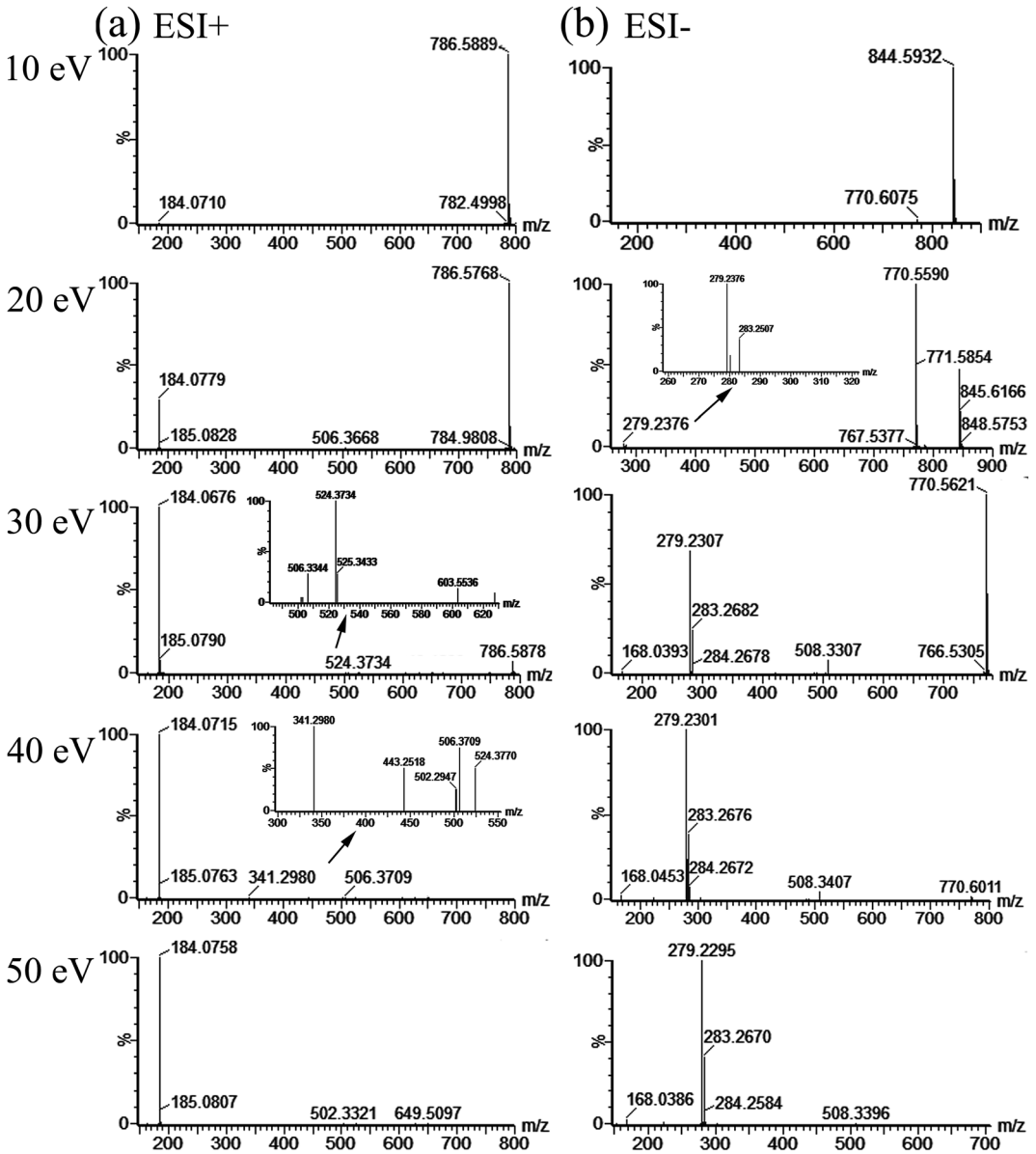

Fig. 6 MS/MS spectra of PC (18 : 0/18 : 2) in ESI (+) (a) and ESI (−) (b) modes at different collision energies (10 eV, 20 eV, 30 eV, 40 eV, and 50 eV).

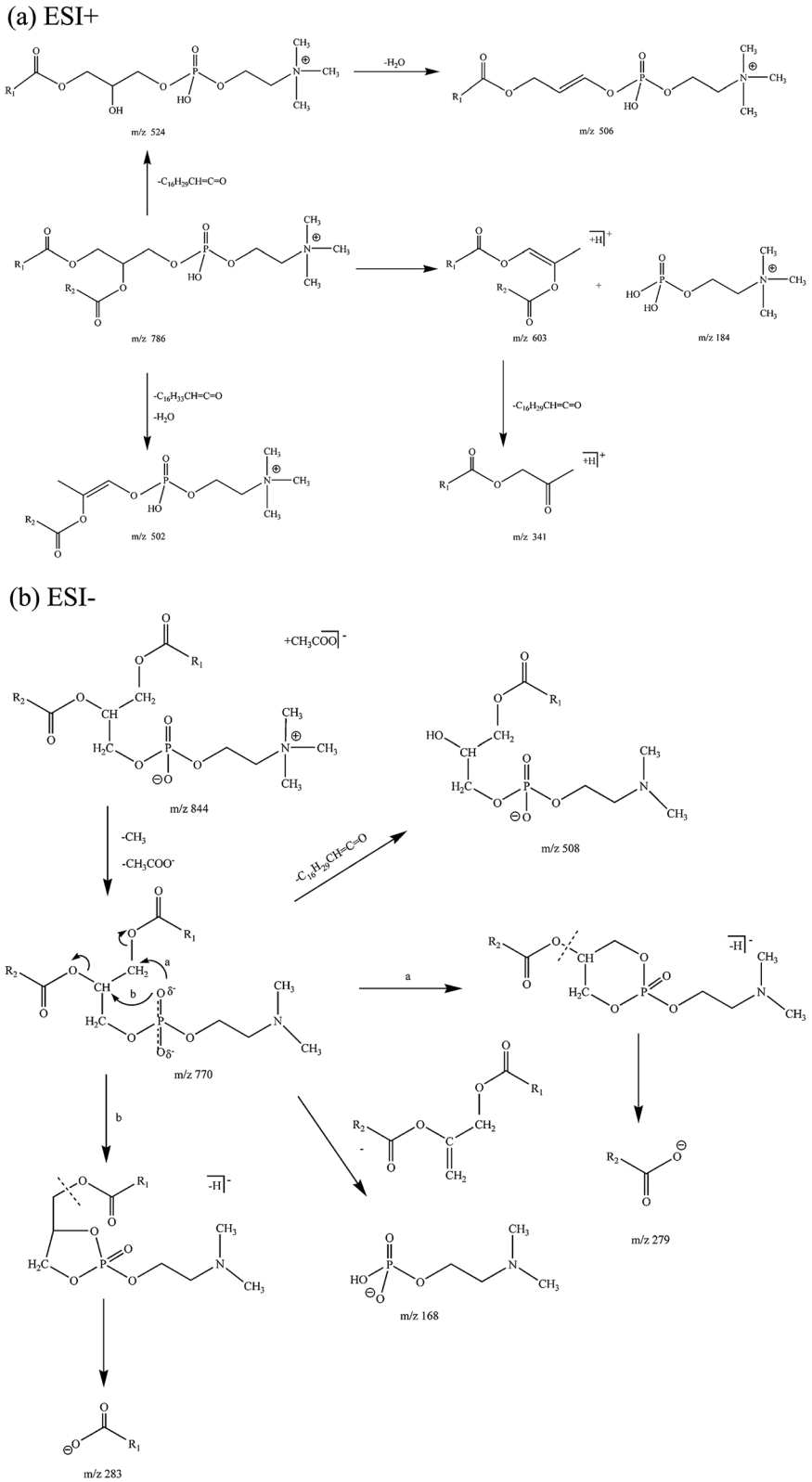

Fig. 7 The fragmentation pathways of PC (18 : 0/18 : 2) in ESI (+) (a) and ESI (−) (b) modes.

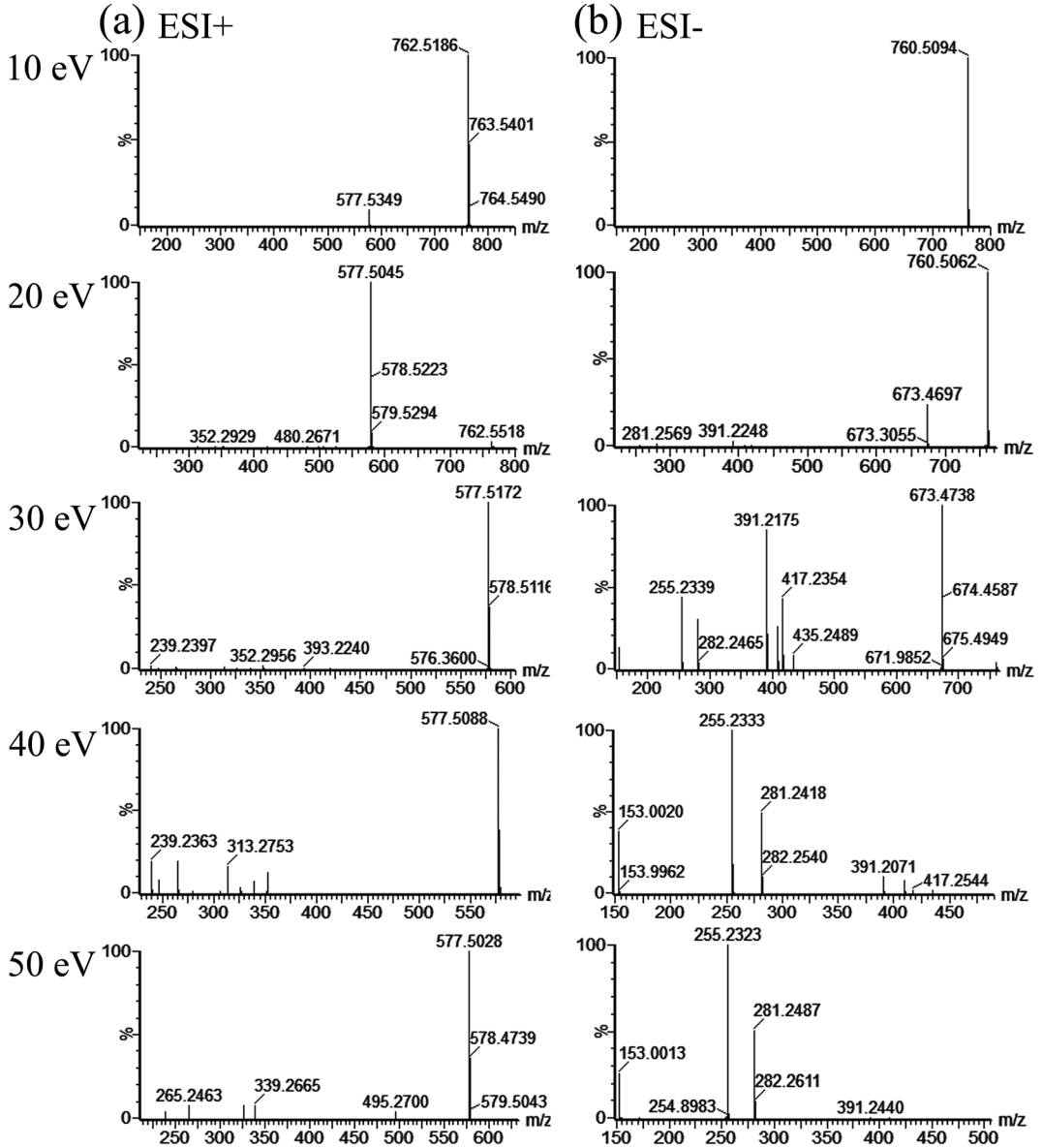

Fig. 8 MS/MS spectra of PS (16 : 0/18 : 1) in ESI (+) (a) and ESI (−) (b) modes at different collision energies (10 eV, 20 eV, 30 eV, 40 eV, and 50 eV).

substituent group of the phosphate head group hindered the attack of the anionic site of the phosphate group at C-1 of the glycerol backbone. PS preferentially formed the six-membered ring transition state and produced a higher intensity of ions at *m*/*z* 255 $[R_1COO^-]^-$. Summing up the above, the abundance ratio of the *sn*-1/*sn*-2 carboxylate anions could provide useful information regarding the positions of the two acyl chains.

3.3 The fragmentation regularity of SM

SM differs from the glycerophospholipids in its chemical structure; it consists of a sphingosine, an acyl chain, and choline. The fragmentation patterns in different ion modes are shown in Fig. 10. In ESI (+) mode, SM (d18 : 1/18 : 0) formed the molecular ion at *m*/*z* 731 $[M + H]^+$ and the characteristic ion at *m*/*z* 184 $[C_5H_{15}O_4NP]^+$. The other daughter ions at *m*/*z* 713 $[731 - H_2O]^+$, 447 $[713 - C_{16}H_{33}CH{=}C{=}O]^+$, 654 $[713 - (CH_3)_3N]^+$, and 530 $[713 - HPO_4CH_2CH_2N(CH_3)_3]^+$ could be detected. In ESI (−) mode, SM (d18 : 1/18 : 0) readily produced ions at *m*/*z* 715 $[M - CH_3]^-$ and adduct molecular ions at *m*/*z* 789 $[M + CH_3COO^-]^-$ when the mobile phase contained acetic acid (shown in Fig. 11). Similar to PC, SM has the same characteristic ion at *m*/*z* 168 $[C_4H_{11}O_4NP]^-$ when the collision energies exceed 30 eV (Fig. 10). It is worth noting that PC and SM, whose polar head groups have similar structures, were difficult to distinguish by only their characteristic daughter ions in ESI (+) or ESI (−) mode. It was found that PC has *sn*-1 and *sn*-2 carboxylate anions with different relative abundances in ESI (−) mode, while SM does not (Fig. 10b); this could be used to distinguish SM and PC.

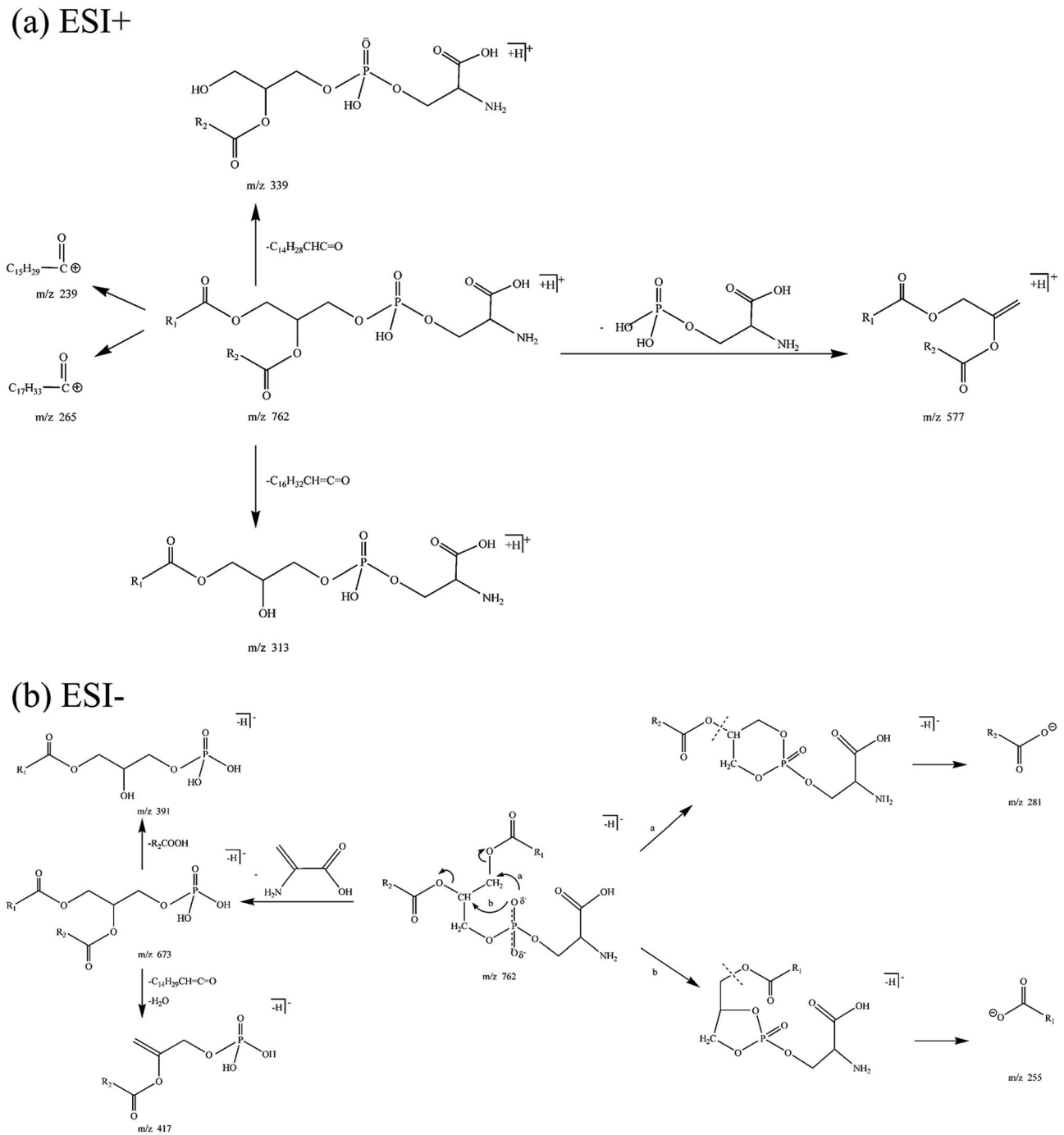

Fig. 9 The fragmentation pathways of PS (16 : 0/18 : 1) in ESI (+) (a) and ESI (−) (b) modes.

3.4 Regular ion patterns of phospholipid standards from MS

The regular ion patterns of five phospholipid standards and the abundance ratios of their *sn*-1/*sn*-2 carboxylate anions in different ion modes were studied through analysis of MS/MS information. As shown in Table 1, different phospholipids can produce characteristic ions and undergo neutral loss associated with fragmentation reactions of their specific polar head groups. PE produced unique daughter ions $[C_2H_7O_4NP]^-$ at *m*/*z* 140 and $[C_5H_{11}O_5NP]^-$ at *m*/*z* 196 in ESI (−) mode, and the daughter ion $[M + H - 141]^+$ due to the neutral loss of $C_2H_8O_4NP$ (141 Da) in ESI (+) mode. The characteristic ions $[C_6H_{10}O_8P]^-$ at *m*/*z* 241 of PI were detected in ESI (−) mode. PC and SM, whose phosphate head groups have the same structure, produced the daughter ions at *m*/*z* 184 $[C_5H_{15}O_4NP]^+$ in ESI (+) mode and *m*/*z* 168 $[C_4H_{11}O_4NP]^-$ in ESI (−) mode. In addition, the molecular ion $[M - H]^-$ of PS

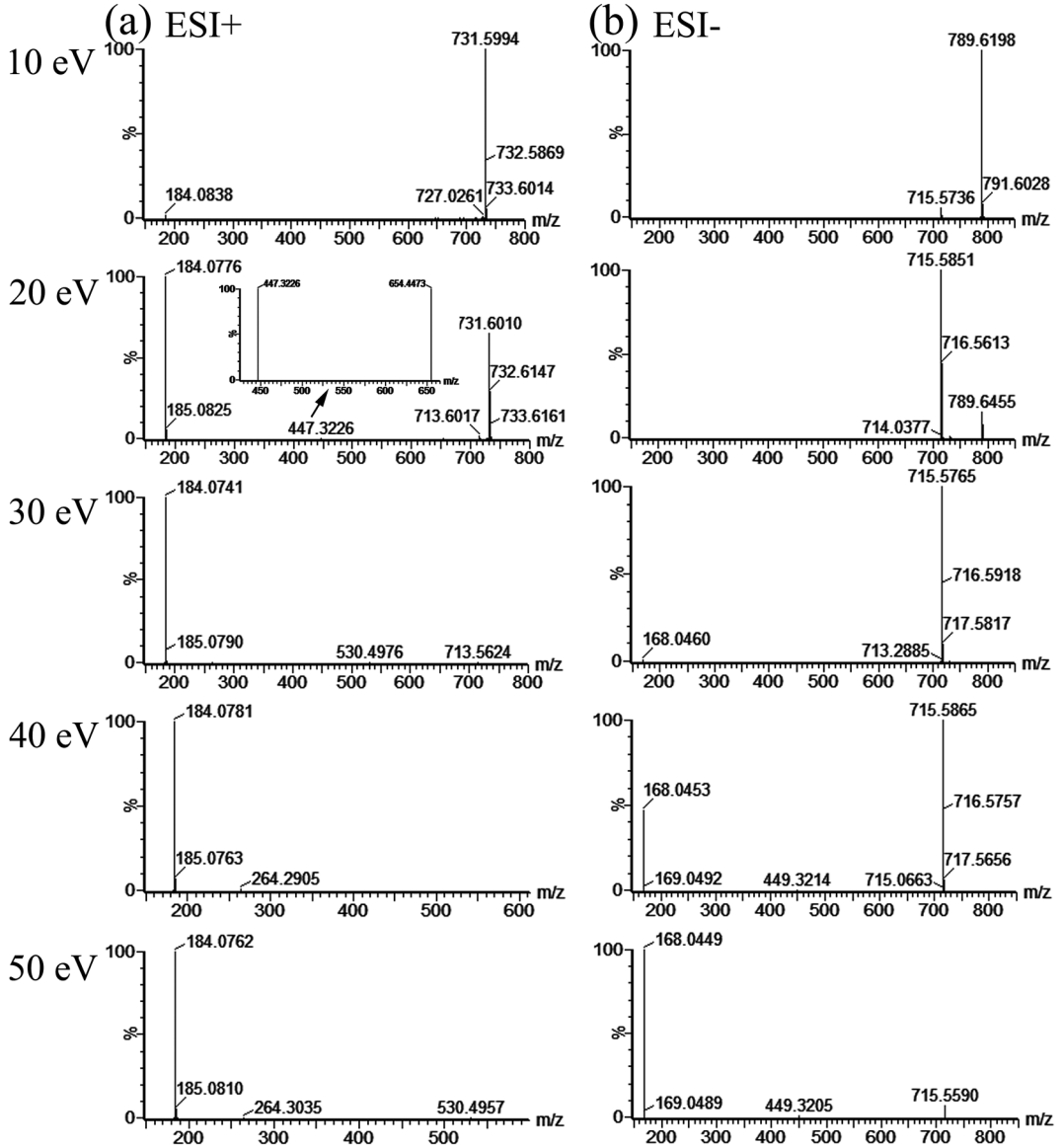

Fig. 10 MS/MS spectra of SM (d18 : 1/18 : 0) in ESI (+) (a) and ESI (−) (b) modes at different collision energies (10 eV, 20 eV, 30 eV, 40 eV, and 50 eV).

could produce the ion $[M - H - 87]^-$ as a result of the neutral loss of its head group $C_3H_5O_2N$ (87 Da). Furthermore, nonspecific ions $[C_3H_6O_5P]^-$ (*m*/*z* 153) were also found; this is a common fragment formed by all glycerol-phospholipids in ESI (−) mode. It was observed that these specific head group fragmentations allowed the specific detection of different phospholipid classes.

3.5 Different patterns of fatty acyl chains of glycerophospholipids

In this work, the different patterns of fatty acyl chains of phospholipids were researched. For example, C20 : 4 of PE (18 : 0/20 : 4) and PI (18 : 0/20 : 4) have patterns of $C_{18}H_{33}CH{=}C{=}O$ and ions at *m*/*z* 303 $[R_2COO^-]^-$, and C16 : 0 of PS (16 : 0/18 : 1) has patterns of ions at *m*/*z* 255 $[R_1COO^-]^-$ and *m*/*z* 239 $[C_{15}H_{29}C{=}O]^+$. Summarizing these five phospholipids and our previous results,[22,23] the fatty acyl chains of glycerophospholipids have three patterns of $[RC{=}O]^+$ in ESI (+) mode, $[RCOO^-]^-$ in ESI (−) mode, and neutral ion R′CH=CO in all ion modes. Among these, R represents long carbon chains and R′ represents carbon chains of 14 Da (–CH_2–) less than R. The fragment patterns and formula weights of common fatty acyl chains contributed to the rapid identification of the type of fatty acyl chains of phospholipids by the fragment ions detected in ESI modes; these are listed in Table 2. Additionally, the ratios of the *sn*-1/*sn*-2 carboxylate anions at different collision energies were used to confirm the positions of carboxylate anions, and are summarized in Table 1.

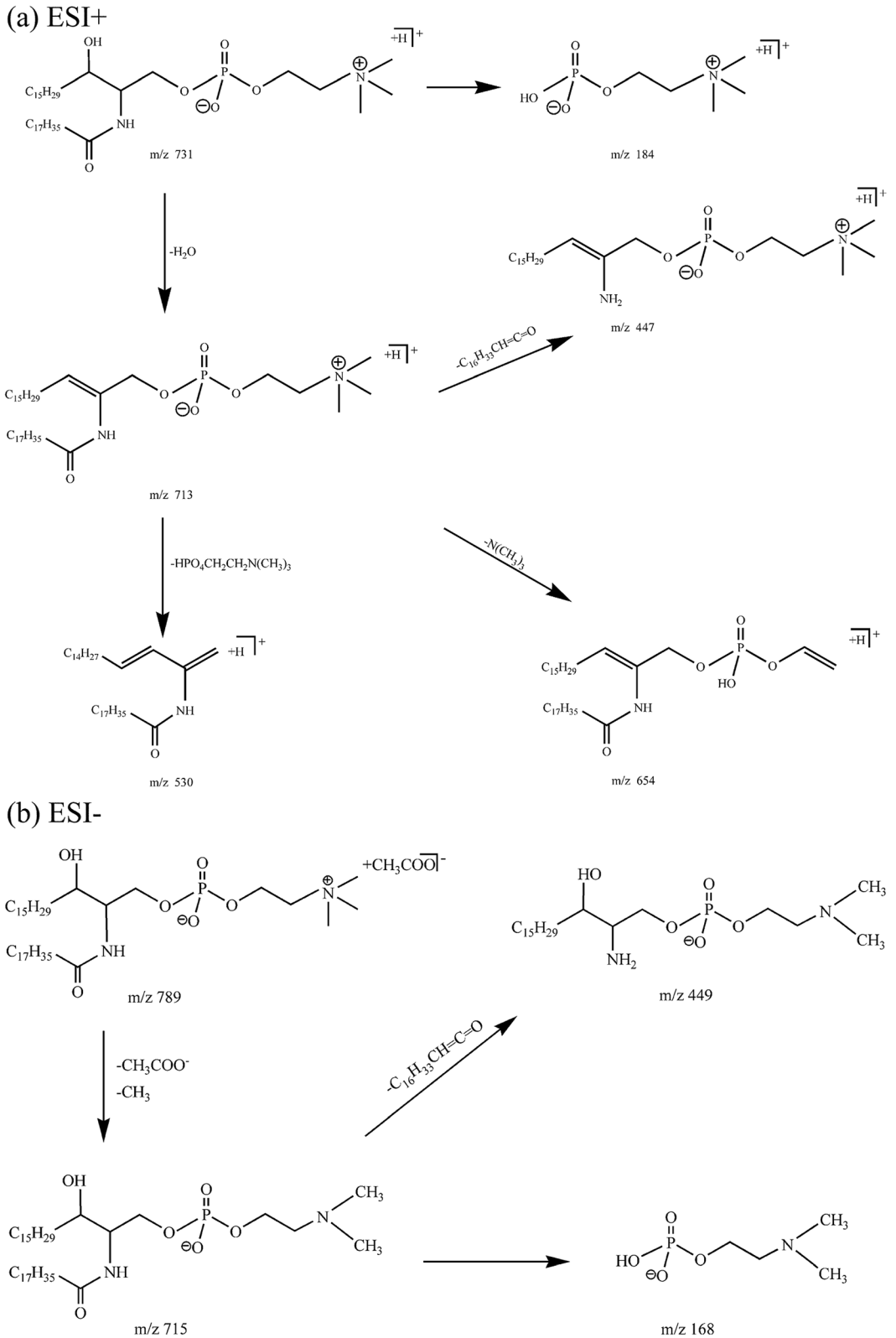

Fig. 11 The fragmentation pathways of SM (d18 : 1/18 : 0) in ESI (+) (a) and ESI (−) (b) modes.

Table 2 Possible ions of the common fatty acyl chains of phospholipids in different ESI modes

Type	ESI (+) $[RC{=}O]^+$ (m/z)	ESI (−) $[RCOO^-]^-$ (m/z)	ESI (±) R′CH=CO (natural loss)	Type	ESI (+) $[RC{=}O]^+$ (m/z)	ESI (−) $[RCOO^-]^-$ (m/z)	ESI (±) R′CH=CO (natural loss)
C12 : 0	183	199	182	C18 : 2	263	279	262
C14 : 0	211	227	210	C20 : 1	293	309	292
C15 : 0	225	241	224	C20 : 3	289	305	288
C16 : 0	239	255	238	C20 : 4	287	303	286
C16 : 1	237	253	236	C20 : 5	285	301	284
C17 : 1	251	267	250	C22 : 1	321	337	320
C18 : 0	267	283	266	C22 : 5	313	329	312
C18 : 1	265	281	264	C22 : 6	311	327	310

4 Conclusions

In this paper, the fragmentation regularities of the five types of phospholipids were studied systematically in different ion modes. Combined with our previous work,[22,23] all these fragmentation regularities were summarized, including three patterns ($[RC{=}O]^+$, $[RCOO^-]^-$ and R′CH=CO) of common fatty acyl chain ions in different ion modes, the variation trend of the ratios of the *sn*-1/*sn*-2 carboxylate anions, and different characteristic ions at different collision energies (10 to 50 eV). These proposed methodologies have already been successfully applied for the high-throughput screening of phospholipid markers in phospholipidomics studies.[12–14] These facts have proved that quick and effective data mining is increasingly necessary, especially with the increasingly abundant information and increasingly growing databases in recent days. The results observed in this paper provide reference tools for the rapid identification of phospholipids and the opportunity to obtain complementary and more comprehensive data in future phospholipidomics studies, which can help minimize or even avoid the risk of lipid loss and misidentification. Although many of the presented observations have already been reported for similar ionization techniques,[20,21,35] such complex information is rarely presented within a single publication based on a strong foundation of experimental application,[22,23] simultaneously covering five lipid categories analyzed in both polarity modes by the use of ESI-Q-TOF-MS. Complete identification can be made by checking our tables and figures. In addition, researchers can list more fatty acyl chain fragmentation ions that are seldom used but which suit their research needs, according to the rules of Table 2.

Acknowledgements

This work was supported by National Science Foundation Project in Guangdong Province (Grant No. 21275036), P. R. China.

References

1 H. Hirschmann, *J. Biol. Chem.*, 1960, **235**, 2762.
2 A. A. Farooqui and L. A. Horrocks, *Neuroscientist*, 2001, **7**, 232.
3 M.-J. Lee, J. R. Van Brocklyn, S. Thangada, C. H. Liu, A. R. Hand, R. Menzeleev, S. Spiegel and T. Hla, *Science*, 1998, **279**, 1552.
4 G. Di Paolo, H. S. Moskowitz, K. Gipson, M. R. Wenk, S. Voronov, M. Obayashi, R. Flavell, R. M. Fitzsimonds, T. A. Ryan and P. De Camilli, *Nature*, 2004, **431**, 415.
5 Y. Takuwa, H. Okamoto, N. Takuwa, K. Gonda, N. Sugimoto and S. Sakurada, *Mol. Cell. Endocrinol.*, 2001, **177**, 3.
6 P. Mattjus, B. Malewicz, J. T. Valiyaveettil, W. J. Baumann, R. Bittman and R. E. Brown, *J. Biol. Chem.*, 2002, **277**, 19476.
7 D. A. Brown and E. London, *J. Biol. Chem.*, 2000, **275**, 17221.
8 A. M. Hodge, D. R. English, K. O'Dea, A. J. Sinclair, M. Makrides, R. A. Gibson and G. G. Giles, *Am. J. Clin. Nutr.*, 2007, **86**, 189.
9 X. Han, D. R. Abendschein, J. G. Kelley and R. W. Gross, *Biochem. J.*, 2000, **352**, 79.
10 N. Attia, N. Domingo, A. M. Lorec, A. Nakbi, S. Hammami, K. Ben Hamda, H. Portugal, D. Lairon, M. Hammami and F. Chanussot, *Clin. Biochem.*, 2009, **42**, 845.
11 R. de Vries, P. J. W. H. Kappelle, G. M. Dallinga-Thie and R. P. F. Dullaart, *Atherosclerosis*, 2011, **217**, 253.
12 L. Liu, M. Wang, X. Yang, M. Bi, L. Na, Y. Niu, Y. Li and C. Sun, *Clin. Chem.*, 2013, **59**, 1388.
13 A. Floegel, N. Stefan, Z. H. Yu, K. Mühlenbruch, D. Drogan, H. G. Joost, A. Fritsche, H. U. Häring, M. Hrabě de Angelis, A. Peters, M. Roden, C. Prehn, R. Wang-Sattler, T. Illig, M. B. Schulze, J. Adamski, H. Boeing and T. Pischon, *Diabetes*, 2013, **62**, 639.
14 C. Zhu, Q. L. Liang, P. Hu, Y. M. Wang and G. A. Luo, *Talanta*, 2011, **85**, 1711.
15 K. Yokoyama, F. Shimizu and M. Setaka, *J. Lipid Res.*, 2000, **41**, 142.
16 T. Sano, D. Baker, T. Virag, A. Wada, Y. Yatomi, T. Kobayashi, Y. Igarashi and G. Tigyi, *J. Biol. Chem.*, 2002, **277**, 21197.
17 A. R. Nor Aliza, J. C. Bedick, R. L. Rana, H. Tunaz, W. W. Hoback and D. W. Stanley, *Comp. Biochem. Physiol., Part A: Mol. Integr. Physiol.*, 2001, **128**, 251.
18 K. Y. Tserng and R. Griffin, *Anal. Biochem.*, 2003, **323**, 84.
19 M. Farré, M. Gros, B. Hernández, M. Petrovic, P. Hancock and D. Barceló, *Rapid Commun. Mass Spectrom.*, 2008, **22**, 41.
20 E. Hvattum, G. Hagelin and A. Larsen, *Rapid Commun. Mass Spectrom.*, 1998, **12**, 1405.
21 X. J. Yan, H. Y. Li, J. L. Xu and C. X. Zhou, *Chin. J. Oceanol. Limnol.*, 2010, **28**, 106.

22 J. J. Pi, X. Wu, S. T. Yang, P. Y. Zeng and Y. F. Feng, *J. Sep. Sci.*, 2015, **38**, 886.
23 Y. Q. She, J. A. Song, E. Yang, L. L. Zhao, Y. M. Zhong, W. Rui, Y. F. Feng and X. Wu, *Biomed. Chromatogr.*, 2014, **28**, 1744.
24 J. F. Brouwers, E. A. Vernooij, A. G. Tielens and L. M. Van Golde, *J. Lipid Res.*, 1999, **40**, 164.
25 E. A. Vernooij, J. F. Brouwers, J. J. Kettenes-Van den Bosch and D. J. Crommelin, *J. Sep. Sci.*, 2002, **25**, 285.
26 R. Taguchi, J. Hayakawa, Y. Takeuchi and M. Ishida, *J. Mass Spectrom.*, 2000, **35**, 953.
27 J. A. Zirrolli, K. L. Clay and R. C. Murphy, *Lipids*, 1991, **26**, 1112.
28 H. Münster and H. Budzikiewicz, *Biol. Chem. Hoppe-Seyler*, 1988, **369**, 303.
29 R. N. A. H. Lewis and R. N. McElhaney, *Chem. Phys. Lipids*, 1998, **96**, 9.
30 J. L. Kerwin, A. R. Tuininga and L. H. Ericsson, *J. Lipid Res.*, 1994, **35**, 1102.
31 P. E. Haroldsen and S. J. Gaskell, *Biomed. Environ. Mass Spectrom.*, 1989, **18**, 439.
32 D. Zhang, X. Chen, Z. Song, X. Yu, T. Zhang and K. Bi, *Zhongnan Yaoxue*, 2010, **8**, 593.
33 K. A. Harrison and R. C. Murphy, *J. Mass Spectrom.*, 1995, **30**, 1772.
34 Y. P. Ho and P. C. Huang, *Rapid Commun. Mass Spectrom.*, 2002, **16**, 1582.
35 J. Godzien, M. Ciborowski, M. P. Martínez-Alcazar, P. Samczuk, A. Kretowski and C. Barbas, *J. Proteome Res.*, 2015, **14**, 3204.

